Mitochondrial complex I deficiency occurs in skeletal muscle of a subgroup of individuals with Parkinson's disease

Simon Ulvenes Kverneng[1,2,3], Kjersti Eline Stige[1,2,3,4,5], Haakon Berven[1,2,3], Sepideh Mostafavi[1,2,3], Katarina Lundervold[1,2,3], Michele Brischigliaro[6,7], Brage Brakedal[1,2,3], Geir Olve Skeie[1,2,3], Irene Hana Flønes[1,2,3], Lilah Toker[1,2,3], Erika Fernandez-Vizarra[6,7], Ragnhild Eide Skogseth[8,9], Kristoffer Haugarvoll[1,2,3], Yamila N Torres Cleuren[1,2,3], Christian Dölle[1,2,3], Gonzalo S Nido[1,2,3], and Charalampos Tzoulis[1,2,3*]

1. Neuro-SysMed, Department of Neurology, Haukeland University Hospital, 5021 Bergen, Norway. 2. Department of Clinical Medicine, University of Bergen, Pb 7804, 5020 Bergen, Norway. 3. K.G. Jebsen Center for Translational Research in Parkinson's disease, University of Bergen, Pb 7804, 5020 Bergen, Norway. 4. The Department of Neuromedicine and Movement Sciences (INB), Norwegian University of Science and Technology (NTNU), 7491 Trondheim, Norway. 5. Department of Neurology and Clinical Neurophysiology, St Olav's University Hospital, 7006 Trondheim, Norway. 6. Department of Biomedical Sciences, University of Padova, 35131 Padova, Italy. 7. Veneto Institute of Molecular Medicine, 35129 Padova, Italy. 8. Department of Geriatric Medicine, Haraldsplass Deaconess Hospital, Bergen, Norway. 9. Department of Clinical Sciences, Faculty of Medicine, University of Bergen, Bergen, Norway

[*]**Correspondence to:**
Prof. Charalampos Tzoulis
Neuro-SysMed Center of Excellence for Clinical Research in Neurological Diseases
Department of Neurology, Haukeland University Hospital
Department of Clinical Medicine, University of Bergen
5021 Bergen, Norway.
Telephone: +47 55975061
E-mail: charalampos.tzoulis@uib.no
E-mail-2: charalampos.tzoulis@helse-bergen.no

Word count main text: 4,322 (excluding abstract, Methods, references and figure legends)

Running title: Complex I deficiency in muscle indicates PD subgroup

Number of figures: 5

Number of tables: 3

Number of supplementary files: 13 figures, 19 tables, 12 data files.

Keywords: Parkinson's disease, parkinsonism, subtypes, subgroups, stratification, mitochondria, mitochondrial respiratory chain, mitochondrial DNA, muscle.

Abstract

Widespread neuronal complex I (CI) deficiency was recently reported to be a characteristic in a subgroup of individuals with idiopathic Parkinson's disease (PD). Here, we sought to determine whether a CI deficient subgroup could be discerned using clinically accessible muscle biopsy. Vastus lateralis needle biopsies were collected from 83 individuals with PD and 29 neurologically healthy controls and analyzed by immunohistochemistry for complexes I and IV, cytochrome c oxidase/succinate dehydrogenase (COX/SDH) histochemistry, and spectrophotometric activity assays of complexes I-IV. Mitochondrial DNA (mtDNA) copy number, deletions, and point variation were analyzed in single muscle fibers and bulk biopsy samples. PD muscle exhibited reduced CI activity at the group level, with 9% of cases falling below two standard deviations of the control group. This deficiency was not associated with mtDNA abnormalities. Our findings support the existence of a PD subpopulation characterized by CI pathology and suggest that stratification by extra-neural mitochondrial dysfunction may be informative for selecting individuals for clinical trials.

Introduction

Parkinson's disease (PD) is a clinicopathologically defined neurodegenerative disorder of unknown etiology[1]. It affects 1-2% of the population above the age of 65 years and its prevalence is rapidly rising, making it one of the fastest growing neurological diseases [2–4]. There are currently no disease-modifying therapies for PD[5,6]. A significant barrier to mechanistic and therapeutic breakthroughs in PD is its heterogeneity. Individuals with PD demonstrate a wide range of clinical presentations, progression rates, and neuropathological signatures[7–9]. This phenotypical diversity has led to the speculation that biological subtypes of PD, beyond the known monogenic forms, may exist, each with its own underlying mechanisms and therapeutic susceptibilities[10–12]. Identifying these subtypes will be pivotal for the development of targeted, disease-modifying interventions for PD[6].

Mitochondrial dysfunction has emerged as a central feature in the pathogenesis and pathophysiology of idiopathic PD[13]. This is supported by multiple findings, including evidence of compromised mitochondrial DNA (mtDNA) maintenance in the dopaminergic *substantia nigra pars compacta* (SNc), and respiratory complex I (CI) deficiency in multiple brain regions, as well as extra-neural tissues of individuals with PD[13–16]. However, recent findings by our group suggest that such mitochondrial abnormalities are not universally present in PD. Rather, a pronounced and widespread neuronal CI deficiency occurs only in a subset of individuals, suggesting a distinct PD subtype, which we have termed CI deficient PD (CI-PD). Based on our observations in post-mortem brain tissue, this group represents ~25% of idiopathic PD cases[17]. The CI-PD subtype may be particularly susceptible to therapeutic interventions targeting mitochondrial function, highlighting the need for stratification biomarkers for clinical trials.

In the current work, we hypothesized that it is possible to identify individuals with CI-PD through analysis of clinically accessible samples. This hypothesis was based on the observation

that previous studies assessing mitochondrial function in peripheral tissue samples of individuals with PD have been highly inconsistent, with approximately half of the studies showing significant difference between PD and healthy control at the group level[16]. While these conflicting findings could be a result of methodological differences and small sample sizes (<30 individuals with PD in most studies)[16], this observed variability raises the possibility that mitochondrial CI deficiency in extra-neural tissue is confined to the CI-PD subgroup. To address this question, we conducted a comprehensive analysis of the quantitative and functional integrity of the MRC in skeletal muscle biopsies of individuals with PD (n = 83) and neurologically healthy controls (n = 29, Fig. 1). We chose skeletal muscle because of its high mitochondrial content and its status as a post-mitotic tissue that accumulates mitochondrial changes over time, similar to neurons[18]. Our study aimed to clarify the extent and nature of mitochondrial dysfunction in skeletal muscle of individuals with PD, potentially paving the way for new diagnostic and therapeutic approaches.

Results

Validation of quadruple immunohistochemistry for quantitative mitochondrial respiratory chain assessment

Quantitative MRC assessment in muscle was performed by quadruple immunohistochemistry for complexes I and IV (CI and CIV), VDAC1 and laminin. CI and CIV levels were normalized to VDAC1, to account for total mitochondrial mass. To assess the validity of our assay, we compared it to cytochrome c oxidase/succinate dehydrogenase (COX/SDH) histochemical staining in serial sections from a skeletal muscle biopsy of an individual with a single mtDNA deletion, exhibiting multiple COX negative fibers (Supplementary Fig. 1). There was a strong correlation between COX positivity and CIV levels in single muscle fibers as assessed by immunohistochemistry (Kendall's $\tau = 0.71$, $n = 60$, $P = 7.81 \times 10^{-12}$, Supplementary Fig. 1h). While there is no reliable histochemical assay to evaluate CI integrity, fibers with CIV deficiency due to mtDNA deletion are often also deficient for CI[19]. In line with this, there was a significant correlation between COX positivity and CI level (Kendall's $\tau = 0.71$, $n = 60$, $P = 7.04 \times 10^{-12}$, $n = 60$, Supplementary Fig. 1i).

Cytochrome c oxidase/succinate dehydrogenase histochemistry shows no complex IV deficiency in PD muscle

Skeletal muscle sections from 68 individuals with PD (46 males, 22 females, mean age 65.9 ± 7.8 years) and 21 neurologically healthy controls (5 males, 16 females, mean age 61.1 ± 9.9 years) were assessed by COX/SDH histochemical staining (Supplementary Fig. 2). The demographic and clinical information of the study cohort is shown in Table 1, while experimental allocation and demographic and clinical information per analysis is shown in Supplementary Data 1 and Supplementary Table 1, respectively. There were generally few COX-negative fibers, ranging between 0-7 per section (Supplementary Data 2). One control

individual had 23 COX-negative fibers, which raised suspicion of mitochondrial disease. This individual was excluded from the study. The proportions of COX-negative or -intermediate muscle fibers per section were not significantly different in the PD and control groups (Supplementary Table 2). Similarly, there was no significant difference between the PD and control groups in the proportion of individuals with any COX-negative or -intermediate muscle fibers (Supplementary Table 2).

Immunohistochemistry shows no quantitative changes of complexes I or IV in PD muscle

We next implemented the quadruple immunohistochemistry assay to assess the level of CI and CIV in skeletal muscle sections from 71 individuals with PD (47 males, 24 females, mean age 66.2 ± 7.8 years) and 21 neurologically healthy controls (5 males, 16 females, mean age 61.1 ± 9.9 years; Supplementary Data 1). In each section, the fluorescence signal was measured in single muscle fibers (n = 75 - 100 per section) to capture inter-fiber variability, as well as in a single large area encompassing the majority of muscle fibers of the section (Supplementary Fig. 3). The two approaches showed high level of correlation at the subject level for both CI ($\rho(90) = 0.97$, $P = 2.2 \times 10^{-16}$) and CIV $\rho(90) = 0.95$, $P = 2.2 \times 10^{-16}$; Supplementary Fig. 4).

Single fiber data were then analyzed using a linear mixed effects model with disease state, age, sex, smoking status, and staining batch as fixed effects, and study subject as a random effect, with the dependent variable log-transformed (Table 2, Supplementary Data 3). At the group level, muscle fibers from cases and controls displayed similar CI and CIV levels (Fig. 2, Supplementary Fig. 5, Table 2). Age was negatively associated with both CI levels (B = -0.002, P = 0.034, Table 2) and CIV levels (B = -0.002, P = 0.026, Table 2). While we did not observe an effect of sex on CI levels, male subjects exhibited significantly higher CIV levels (B = 0.052,

P = 0.003, Table 2). Single fiber VDAC1-fluorescence showed similar distribution and levels in the PD and control groups, indicating similar mitochondrial content, and was not significantly associated with age, sex, or smoking status (Supplementary Fig. 6, Supplementary Table 3). Analysis of the measurements taken from large areas of the sections, encompassing the majority of muscle fibers from each sample, yielded similar results (Supplementary Table 4, Supplementary Data 4).

Complex I activity is reduced in PD muscle

The specific enzymatic activities of MRC complexes I-IV (CI-CIV) and citrate synthase (CS) were measured in muscle biopsy samples. Active smokers were omitted because smoking is known to inhibit mitochondrial respiration[20], and in particular CI function [21–24]. After removal of two outliers (Methods; Supplementary Data 5), the dataset consisted of 57 individuals with PD (35 males and 22 females, mean age 67.1 ± 7.4 years) and 25 controls (8 males and 17 females, mean age 65.4 ± 12.0 years; Supplementary Data 1). Data were analyzed using a linear regression model with disease state, age, sex, and measurement batch as independent variables, and with the dependent variable log-transformed (Table 3, Supplementary Data 5). CS activity, reflecting mitochondrial mass, showed no significant difference between individuals with PD and controls or association with any of the covariates. In contrast, CI activity normalized by CS activity (CI/CS) was significantly lower in the PD group compared to the controls (B = -0.079, P = 0.008), and remained significant after controlling for multiple testing (P = 0.032), while the CS-normalized activities of CII-IV (CII-IV/CS) showed no significant differences (Fig. 3, Supplementary Fig. 7, Table 3, Supplementary Table 5a). The MRC complex activities were not influenced by age or sex, with the exception of CIII, which showed a positive association with age (B = 0.008, P = < 0.001, Table 3). The regression coefficient was back-transformed from log for interpretation. This revealed a 17% lower CI/CS in the PD group compared to

controls, corresponding to a medium effect size (Cohen's *d*) of 0.65. Similar results were observed when smokers were included in the analysis (Supplementary Figure 8, Supplementary Figure 9, Supplementary Table 5b), although in this case the difference in CI/CS between the PD and control group did not remain significant after controlling for multiple testing.

Since previous results in PD muscle have been conflicting, we performed a power calculation based on our observed effect size (Cohen's *d*) of 0.65, to estimate the power of discovery as a function of sample size. This showed that using a Student's *t*-test, a total sample size of $n = 78$ or $n = 103$ would be required to detect a significant difference between cases and controls at a two-sided significance level of 5% and power of 80% or 90%, respectively. A plot of power as a function of sample size is shown is Supplementary Fig. 10.

CI/CS activity data were further analyzed within the PD group to investigate associations with disease severity. Linear regression revealed no association between CI/CS activity and the International Parkinson and Movement Disorder Society Unified Parkinson's Disease Rating Scale (MDS-UPDRS) part III score, Montreal Cognitive Assessment (MoCA) score, disease duration, sex or age (Supplementary Table 6).

Reduction of complex I activity is not pervasive in PD

We next investigated the distribution of CI/CS activity, to determine the pervasiveness of CI deficiency in PD muscle. Plotting the activity after regressing out the batch effect, revealed a substantial overlap between the PD and control groups (Fig. 3a). Out of 57 individuals with PD, 9 (15.8%) displayed CI/CS activity below the range of controls. Using a more stringent criterion, whereby abnormal CI/CS activity was defined as falling below 2 standard deviations of the control group, 5 out of 57 (8.8%) were classified as CI deficient. These individuals

showed a mean decrease in CI/CS activity by 24.5% (range 17.8-29.1%) compared to the mean of controls.

Compared to the subgroup with CI/CS activity within the range of controls, the group with low CI/CS activity showed a significant female preponderance (Fisher's exact, $P = 0.020$). However, this did not remain significant after adjusting for multiple testing. There were no differences between the subgroups in terms of age of onset, cognitive function measured by Montreal Cognitive Assessment (MoCA), or motor function measured by MDS-UPDRS III. Moreover, there was a similar number of cases with tremor dominant and postural instability/gait difficulty phenotypes. None of the individuals with activity below the range of controls reported agricultural work, while a single individual reported previous pesticide exposure. These results are summarized in Supplementary Table 7.

In light of the CI/CS activity findings, the CI immunohistochemistry data were re-analyzed, including only subjects from whom both activity- and immunohistochemistry data were available (45 individuals with PD and 17 controls). At the group-level, there was still no significant difference in CI levels between the PD and control group (Supplementary Table 8). To assess whether the decrease in CI/CS activity could be explained by a reduction in CI quantity, we compared the goodness of fit of a model predicting CI/CS activity with and without including the CI immunohistochemistry data. ANOVA between the two models indicated that inclusion of the CI quantity data significantly improved the goodness of fit of the model ($P = 0.002$, Supplementary Table 9). Furthermore, there was a highly significant positive association between CI activity and quantity ($B = 0.806$, $P = 0.002$, Supplementary Table 10).

Single muscle fiber mitochondrial DNA profile shows no difference between PD and controls

Next, we assessed whether PD muscle harbored qualitative or quantitative changes in mtDNA at the single fiber level. A total of 223 single muscle fibers were analyzed from six individuals with PD (5 males and 1 female, mean age 66.8 ± 6.5 years), spanning the CI level range, and six controls (1 male and 5 females, mean age 64.8 ± 9.5 years; Supplementary Fig. 11, Supplementary Data 1). In each fiber, CI and CIV levels were determined using quadruple immunohistochemistry, and mtDNA copy number and deletion fraction were assessed by quantitative PCR (qPCR). Additionally, 157 of these fibers were analyzed for sequence variation by deep sequencing.

We found no difference between the PD and control groups in terms of muscle fiber mtDNA copy number or the proportion of molecules containing major arc deletions (Figure 4a-b, Supplementary Data 6). Likewise, using a linear mixed effects model with study subject as a random effect, we found no association between mtDNA copy number or deletion levels and disease status, (Supplementary Table 11-12). Overall, there was a positive correlation between mtDNA copy number and VDAC1 immunofluorescence ($\rho(221) = 0.38$, $P = 8.6 \times 10^{-9}$), indicating that mtDNA copy number reflected mitochondrial content. This was evident in both the PD ($\rho(109) = 0.33$, $P = 3.8 \times 10^{-4}$) and control ($\rho(110) = 0.39$, $P = 2.5 \times 10^{-5}$) groups. Furthermore, mtDNA copy number showed a positive correlation with the levels of CI ($\rho(221) = 0.21$, $P = 0.0020$) and CIV ($\rho(221) = 0.36$, $P = 5.2 \times 10^{-8}$). Single fiber mtDNA deletion levels were generally low (Fig. 4b) and showed no correlation with the levels of CI ($\rho(221) = -0.017$, $P = 0.800$) or CIV ($\rho(221) = -0.047$, $P = 0.487$).

To determine the presence of point mutations, mtDNA was amplified and sequence variation was assessed in two amplicons covering most of the mtDNA length. This was done using ultra-deep sequencing at a target depth of 100,000x in 157 of the same muscle fibers used for copy number and deletion analyses (Fig. 4c-f, Supplementary Data 7, Supplementary Data 8). The two amplicon regions were analyzed separately due to different mean depth of coverage (mean depth amplicon 1: $1.66\times10^4 \pm 1.01 \times10^4$; amplicon 2: $6.80\times10^4 \pm 1.51\times10^4$; $P < 10^{-15}$, paired Wilcoxon singed rank test). Single fibers exhibited a median of 14 and 16 heteroplasmic positions at levels above 1% in amplicon 1 and 2, respectively. The heteroplasmic load (i.e., the sum of all heteroplasmic levels across each amplicon) was not associated with disease status, age, sex, or with per-fiber CI levels (Supplementary Table 13).

Functional complex I deficiency in PD muscle is not associated with mitochondrial DNA variation

Since the MRC activity measurements had been performed in bulk tissue, we also assessed mtDNA in bulk muscle tissue from 27 individuals, comprising PD with CI activity similar to controls ($n = 8$), PD with low CI activity ($n = 9$), and controls ($n = 10$; Supplementary Fig. 12, Supplementary Data 1). The three groups were matched for age (Supplementary Table 1). There was no significant difference in mtDNA copy number or deletion fraction between PD individuals with either normal or low CI activity and the control group (Fig. 5a-b, Supplementary Table 14, Supplementary Data 9). Similarly, there was no significant difference between the PD group with normal or low CI activity in terms of mtDNA copy number or deletion fraction (Supplementary Table 14). Compared to the results in single fibers, the analyses for sequence variation in bulk muscle revealed very few heteroplasmic positions (mean of 0.33 and 1.00 heteroplasmic sites per sample in amplicon 1 and 2, respectively; Fig. 4c-f, Supplementary Data 10, Supplementary Data 11). Most samples displayed a single

263 heteroplasmy above 1 % or none at all (26/27 and 19/27 samples showed one or no
264 heteroplasmic positions in amplicon 1 and 2, respectively). There was no significant difference
265 in heteroplasmic load between the three groups (amplicon 1: $P = 0.421$, Kruskal-Wallis $\chi^2 =$
266 1.73; amplicon 2: $P = 0.111$, Kruskal-Wallis $\chi^2 = 4.40$). Finally, there was no association
267 between heteroplasmy load and CI activity (Supplementary Table 15).

Discussion

In this work, we sought to explore the prevalence of mitochondrial dysfunction in skeletal muscle of individuals with PD, an area marked by conflicting findings from previous research[16]. Our central hypothesis, based on our recent findings in brain tissue[17], was that MRC dysfunction, specifically in the form of CI deficiency, may occur in a distinct subpopulation of individuals with PD. To increase the power and validity of our analyses compared to earlier research, we employed a much larger cohort (n = 112) than previously reported[16], and obtained our samples from a well-characterized cohort of clinically verified PD and neurologically healthy controls.

We show that most individuals with PD exhibit no signs of quantitative or functional MRC alterations in their skeletal muscle. Conversely, MRC deficiency in the form of a functional CI defect occurs in a subset of cases. This subgroup accounted for approximately 9-16% of our population-based cohort, depending on where the threshold was set. While there was no significant difference in CI levels between PD and controls at the group level, we found a positive association between CI quantity and function. Thus, we cannot exclude that the observed functional defect may be, in part, mediated by a quantitative reduction of the complex.

Our findings explain the conflicting nature of previous results. Earlier studies of MRC function in muscle employed small samples sizes, ranging from 3 to 27 individuals with PD[16]. As shown by our data, these were generally underpowered for detecting CI deficiency. In further support of this, several previous studies reporting MRC dysfunction in PD muscle show a considerable overlap between the PD and control groups, with only a subset of cases displaying a clear reduction of CI activity levels, similar to our results[25–27]. Technical methodological differences may also contribute to variability among studies[16].

The notion that skeletal muscle mitochondrial function is impaired only in a small subset of individuals with PD is further supported by previous in vivo ^{31}phosphorus magnetic resonance spectroscopy (^{31}P-MRS) studies. A study in forearm muscle reported a high (> 2 SDs above the mean of controls) inorganic phosphate / phosphocreatine (Pi/PCR) ratio, indicative of impaired mitochondrial bioenergetic status, in a subset of 9 out of 28 individuals with PD (32%)[28]. Additionally, evidence of mitochondrial dysfunction in the form of lower maximum mitochondrial ATP production (ATPmax) has been found by ^{31}P-MRS in the tibialis anterior muscle of individuals with PD[29]. Notably, ATPmax displayed substantial overlap with the control group, with only 2 out of 29 individuals with PD (7 %) displaying levels < 2SDs of the mean of the controls.

Studies in other extra-neural tissues have also shown highly variable results, with some reporting MRC deficiencies and some not. A thorough assessment of the available data reveals a similar picture to our results in skeletal muscle, i.e., a substantial overlap between the PD and control groups, with a minority of PD cases falling below the range of controls. Studies in platelets that report deficiency of CI activity show a variable decrease of approximately 16-51% when comparing PD and controls at the group level, but with a considerable overlap between the PD and control groups, suggestive of a subgroup with deficiency[30–34]. In contrast to our analyses in skeletal muscle, some of these studies report functional impairment in the other MRC complexes as well[31,33,34]. Studies in skin fibroblasts have shown similar heterogeneity, with impaired mitochondrial function present only in a subset of cases[35–37]. One of these studies reported indirect evidence of impaired mitochondrial respiration by means of decreased mitochondrial membrane potential in a subset of 5% of their PD cohort, using 2 standard deviations of the control group as a reference level of normal mitochondrial membrane potential[35]. Studies in PD lymphocytes that report mitochondrial dysfunction have been

318 contradictory with one study reporting CI deficiency in 3/16 individuals with PD (19%)[38], while
319 another showed decreased CI activity in all the analyzed (20/20) individuals with PD[39]. These
320 studies reported variable deficiency of CIV as well.
321
322 Whether the observed reduction of CI activity in the muscle of individuals with PD relates to
323 the primary pathophysiology of the disease, or is a secondary phenomenon induced by factors
324 such as altered mobility or drug treatment, cannot be ascertained by our study. However, the
325 fact that we did not observe a significant association between CI activity and disease duration
326 suggests that it is not secondary to immobility or dopaminergic treatment. The latter is
327 supported by a study in platelets reporting no effect of the initiation of carbidopa/levodopa and
328 selegiline treatment on CI activity[40], and in rat skeletal muscle, showing that MRC activity was
329 not altered by levodopa treatment[41]. In line with this, CI deficiency has also been reported in
330 platelets and lymphocytes of drug naïve individuals with PD[34,38].
331
332 The mechanisms mediating functional CI deficiency in PD muscle remain unknown. Although
333 we found a positive association between CI quantity and function, we did not detect a significant
334 reduction of CI quantity in muscle tissue of individuals with PD. This is in contrast to the PD
335 brain, which demonstrates both a quantitative reduction and functional deficiency in CI[42].
336 Moreover, the dysfunction is not attributable to qualitative or quantitative alterations in
337 mtDNA, as our analysis showed no correlation with mtDNA copy number, deletion levels, or
338 point mutations. One contributing factor may be genetic variation in one or more of the 37
339 nuclear encoded CI subunits and/or factors required for CI assembly. No individual variants[43],
340 or polygenic enrichment of rare coding variants[44,45] in these genes have been associated with
341 PD. However, an association of PD with a high polygenic score of common variants in genes
342 related to oxidative phosphorylation (OXPHOS) was recently reported[46]. This polygenic score

was found to be associated with altered respiratory function in fibroblasts and induced pluripotent stem cell-derived neuronal progenitors from patients, but no specific CI defect was shown. Furthermore, individuals with high OXPHOS polygenic score had an earlier age of onset, a feature not observed in our CI deficient subgroup. Our findings could be attributable to exposure to environmental inhibitors of CI. Adequately characterizing the exposure to CI inhibitors is challenging, as many and diverse natural and synthetic compounds are known inhibitors[47]. While our results did not indicate a connection with agricultural work or a documented history of pesticide exposure, the possibility of dietary pesticide exposure remains unaccounted for. Given the established link between pesticide exposure and PD[48], further investigation into this area is warranted[49].

Our study has certain limitations that must be taken into consideration. The needle biopsy approach used to obtain the muscle samples has the benefit of reduced invasiveness, compared to an open muscle biopsy, making it feasible to perform on a large number of subjects. However, due to the low amounts of biopsy material with this method, we were not able to perform both the immunohistochemistry and enzymatic activity assays in all study subjects (Supplementary Data 1). While the PD and control groups were well matched for age, they were unbalanced in terms of sex, with a male to female ratio of ~1.9 in the PD group and ~0.4 in the control group. This is mainly because PD has a higher prevalence in males[50], and most control individuals were recruited among the spouses of the individuals with PD. Since our immunohistochemistry assay targeted individual subunits of CI and CIV, we cannot exclude defects of complex/supercomplex assembly and/or altered subunit composition as the cause of deficient function. Investigating this would require analyzing the assembly status of the MRC complexes using methods such as blue native gel electrophoresis and complexome profiling[51,52]. In this study, it was not possible to perform these additional analyses due to the

limited quantity of muscle available to us. Finally, the individuals with PD included in this project have not been genetically characterized. The prevalence of monogenic PD in Norway is very low, estimated at approximately 0.5% and virtually accounted for by *LRRK2* mutations, based on a population-representative cohort from the region of origin of the majority of our samples (Western Norway)[53]. Thus, it is highly unlikely that any significant number of monogenic PD cases was included in our cohort. *GBA* variation, which is more common[54], may be of relevance and this should be explored in future studies. However, since the original neuronal CI deficient subpopulation of PD was found in a genetically characterized sample of idiopathic PD, it is generally unlikely that this subgroup is driven by monogenic contributions.

In summary, regardless of its etiology and pathogenic contribution, our findings confirm the hypothesis that CI deficiency in skeletal muscle is not a pervasive feature of PD, but one that occurs only in a subset of cases. Whether these are the same as (or overlap with) the approximately 25% of the PD cases with widespread neuronal CI deficiency in the post-mortem brain[17], remains to be determined. Interestingly, individuals with PD exhibiting low CI activity in muscle were predominantly females, a trend also exhibited by the subgroup with neuronal CI deficiency[17]. However, unlike the subgroup with neuronal CI deficiency, individuals with low muscle CI activity did not exhibit a predilection for a non-tremor dominant motor phenotype. Determining whether CI deficiency in PD muscle reflects the status of the brain will require examination of muscle and brain tissue from the same individuals. To the best of our knowledge, such a material is not currently available. However, the vast majority of the individuals with PD and controls in the STRAT-PARK cohort[55], where most of our muscle samples originate from, have consented to post-mortem brain donation. Thus, we hope to answer this pertinent question in the future. In the meantime, the applicability of muscle CI deficiency as a clinical stratification biomarker is limited by the invasiveness of the muscle

biopsy, even with our percutaneous technique[55]. Examination of the respiratory chain integrity in more easily accessible samples, such as blood platelets or PBMCs, is warranted to establish whether classification of PD according to mitochondrial pathology can be achieved with more efficient and less invasive testing.

Methods

Cohort characteristics

Clinical data and skeletal muscle biopsies were collected from 83 individuals with PD participating in the NADPARK study[56] ($n = 25$) or the STRAT-PARK cohort[55] ($n = 58$), as well as 29 neurologically healthy controls participating in the STRAT-PARK cohort ($n = 23$) or the STRAT-COG cohort ($n = 6$). Only baseline samples were included from NADPARK participants who received active intervention. STRAT-PARK and STRAT-COG are longitudinal cohort studies of PD and dementia, respectively. Inclusion and exclusion criteria for the studies are provided in Supplementary Tables 16-18. All individuals with PD had a clinical diagnosis of established or probable PD, according to the Movement Disorders Society Clinical Diagnostic Criteria[1], as well as [^{123}I]FP-CIT single photon emission CT (DaTscan) with evidence of nigrostriatal degeneration. Because NADPARK participants were drug naïve at the time of biopsy, the clinical diagnostic criteria for these individuals were re-evaluated after initiation of dopaminergic treatment. Clinical assessment of individuals with PD included a medical history, a complete neurological examination, and the International Parkinson and Movement Disorder Society Unified Parkinson's Disease Rating Scale (MDS-UPDRS) parts I-IV[57]. Classification into tremor dominant (TD) and postural instability/gait difficulty (PIGD) phenotypes was based on MDS-UPDRS scores[58]. Additionally, Montreal Cognitive Assessment (MoCA) scores[59], occupational history, and self-reported data on pesticide exposure were available from STRAT-PARK participants. Demographic and clinical characteristics (mean values) of the participants are provided in Table 1 and Supplementary Table 1. The study was approved by the Regional Committee for Medical and Health Research Ethics, Western Norway (NADPARK: 2018/597, STRAT-PARK: 74985, STRAT-COG: 216664). Written informed consent was obtained from all study participants.

422 **Skeletal muscle biopsy**

423 A needle biopsy of the vastus lateralis muscle was performed using a Bard Magnum biopsy
424 instrument (BD©, United States) with 12Gx10 cm biopsy needle. Biopsies were dissected to
425 remove non-muscle tissue (e.g., fat or fascia) before immediate freezing using isopentane pre-
426 cooled in liquid nitrogen. Samples were stored at -80°C until further analysis.

427

428 **Quadruple immunohistochemistry**

429 The quadruple immunohistochemistry protocol was adapted from Rocha *et al.*[60]. Using a
430 cryotome (CM1950, Leica Biosystems), a transverse section of 12 µm thickness from each
431 frozen biopsy was prepared onto glass slides and left to air dry for 60 minutes. Fixation was
432 then achieved by immersion in 4% paraformaldehyde in PBS for 15 minutes at room
433 temperature before rinsing with distilled water and permeabilizing and dehydrating by
434 immersing in a series of methanol solutions (70% for 10 min; 95% for 10 min; 100% for 20
435 min, followed by 95% for 10 min; 70% for 10 min, and washing in TBS-T (0,1% Tween20 in
436 TBS) for 5 min). Bovine serum albumin (4% in PBS) was then applied for 15 minutes to prevent
437 non-specific binding. Subsequently, a cocktail of four primary antibodies diluted in TBS-T was
438 applied, directed against VDAC1 (an outer mitochondrial membrane voltage-dependent
439 channel, Abcam, #ab14734), NDUFB10 (a subunit of CI of the MRC, Abcam, #ab196019),
440 MTCO1 (a subunit of CIV of the MRC, Invitrogen, #459600), and laminin (a basement
441 membrane glycoprotein, Sigma-Aldrich, #L8271). Staining was carried out in two batches,
442 using the same working solutions of antibodies and reagents for all samples within the same
443 batch. The samples in each batch were divided between three technicians who each included a
444 negative control (no primary antibody). Primary antibodies were incubated for 1 hour at room
445 temperature. Following a washing step of TBS 2 x 5 min and TBST 1 x 5 min, a cocktail of
446 four secondary fluorescent antibodies (Alexa Fluor™ 488 anti-mouse IgG2b, Invitrogen, #A-

21141; Alexa Fluor™ 594 anti-rabbit IgG, Invitrogen, #A-11012; Alexa Fluor™ 647 anti-mouse IgG2a, Invitrogen, #A-21241; DyLight™ 405 anti-mouse IgG1, BioLegend, #409109) diluted in TBS-T was applied and incubated in the dark for 1 hour at room temperature. Sections were then washed in TSB-T 2 x 5 min and rinsed with TBS before mounting with ProLong™ Diamond Antifade Mountant (Invitrogen, #P36961). Following staining with secondary antibodies, sections were kept in the dark until image acquisition. For validation of the immunohistochemistry assay, a muscle biopsy was used from an individual with mitochondrial myopathy due to a single mtDNA deletion and known CI and CIV deficiency (Supplementary Data 12).

Image acquisition and fluorescence quantification

Fluorescent images were acquired at 40 x magnification on a slide scanner (Olympus VS120 S6) and VS-ASW-S6 software, with a Hamamatsu ORCA-Flash 4.0. V3 B/W camera for fluorescence imaging, using a quad filter (DAPI, FITC, TRITC & CY5, Supplementary Table 19) for fluor dyes at 405 nm (laminin), 488 nm (VDAC1), 596 nm (NDUFB10) and 647 nm (MTCO1). Exposure times were maintained for all channels between samples. Images were acquired at 16-bit. Image processing and quantification of fluorescence intensity were performed in ImageJ (ImageJ2, version 2.3.0/1.53f). Using the laminin signal, a mask was created to separate individual muscle fibers (Supplementary Fig. 3 and 13). In cases with poor laminin staining, the mask was created manually. Fluorescence intensity ("mean gray value" in the ImageJ software) was measured in 100 individual muscle fibers per muscle section, apart from seven sections where only 75-95 fibers were measured due to biopsy size. In addition, global fluorescence intensity was also measured in larger areas encompassing most of the muscle section (Supplementary Fig. 3). Non-muscle tissue, such as blood vessels and connective tissue, was manually removed from the region of interest in a filtering step. The

final region of interest was then generated by adjusting a threshold on the VDAC1-signal so that any defects in the tissue caused by thawing or sectioning were excluded. All fluorescence measurements were adjusted for background signal by subtracting the signal intensity acquired from a negative control belonging to the same batch and the same technician. Some sections were scanned twice due to technical adjustments of the slide scanner. This did not have a significant effect on fluorescence intensity levels when added to statistical models. The number of scans per section was therefore omitted as a variable from the final analysis of the fluorescence dataset.

Cytochrome c oxidase/succinate dehydrogenase histochemical staining

COX/SDH histochemical staining was used to identify COX-negative (CIV negative) muscle fibers. In this assay, COX-positive fibers appear as brown, while COX-negative fibers exhibit a blue stain due to intact SDH (CII) activity[61]. Transverse sections of 12 µm thickness were prepared as described above in the section "Quadruple immunohistochemistry". Sections were left to air dry for 60 minutes before incubating with ~125 µl of COX-staining solution (prepared by combining 800 µl 5mM diaminobenzidine tetrahydrochloride and 200 µl 500 mM cytochrome C mixed with a few grains of catalase) for 45 minutes at 37°C. After washing in PBS for 3 x 5 minutes, sections were incubated with ~125 µl of SDH staining solution (prepared by combining 800 µl 1.875mM nitroblue tetrazolium (NBT), 100 µl 1.3 M sodium succinate, 100 µl 2 mM phenazine methosulphate and 10 µl 100mM sodium azide) for 40 minutes at 37 °C. Finally, sections were washed in PBS for 3 x 5 minutes before dehydration in a graded ethanol series (75% for 1 minute, 95% for 1 minute, and 100% for 10 minutes) and mounting. Brightfield images were acquired with a slide scanner (Olympus VS120 S6) and COX-status for single muscle fibers was qualitatively assessed ("positive", "intermediate" or "negative") by two readers (SUK and CT).

497

498 **Mitochondrial respiratory chain enzymatic activity measurements**

499 5-10 mg of a muscle biopsy was cut in small pieces using a surgical scalpel. The tissue was
500 then homogenized in a glass-glass Dounce type potter using 20 volumes of Medium A (0.32 M
501 sucrose, 10 mM Tris-HCl pH 7.4, 1 mM EDTA) and 15 manual strokes. The homogenate was
502 transferred to an Eppendorf tube and centrifuged at 800 x g for 5 minutes at 4ºC. The pellet was
503 discarded, and the supernatant was collected, transferred to a clean tube and immediately frozen
504 at -80ºC. These mitochondria-enriched fractions were kept at -80ºC overnight. Before
505 performing the measurements, the samples were thawed at 37ºC and snap-frozen again in liquid
506 nitrogen. This freeze-thawing cycle was carried out twice. The activity measurements of the
507 each of respiratory chain complex activities and the citrate synthase activity were performed
508 using 10-30 µl of mitochondria-enriched supernatant, in a total reaction volume of 200 µl, using
509 a plate-reader spectrophotometer as described.[62] One PD sample and one control sample
510 exhibited unusually high values of specific CS activity, and were removed from the dataset as
511 outliers (Supplementary Data 5).

512

513 **Laser microdissection and sample lysis**

514 Six PD samples and six control samples were selected for laser microdissection of single muscle
515 fibers to cover the spectrum of median single fiber VDAC1-adjusted CI level (Supplementary
516 Fig. 11, Supplementary Data 1). Two serial sections of 12 µm were prepared from each biopsy.
517 One was subjected to quadruple immunohistochemistry staining as described above, while the
518 other one was placed on a membrane slide 2.0 µm PEN (Leica Microsystems, #11505158), air-
519 dried for 30 minutes and stained with hematoxylin before dehydration in ascending (70%, 95%,
520 and 100%) ethanol solutions. Microdissection was performed on a laser microdissection
521 microscope (Leica LMD7). Individual muscle fibers were collected in reaction tubes and lysed

in 20 µl of lysis buffer (50 mM TrisHCl pH 8.0, 0.5% Tween20, 190 µg/mL proteinase K, diluted in sterile purified water) overnight at 56°C. Samples were then centrifuged at 2000 x g for 10 minutes at room temperature before incubation at 95°C for 10 minutes to inactivate proteinase K. Finally, samples were cooled on ice before one last centrifugation step at 2000 x g for 2 minutes at room temperature. During microdissection, the location of each dissected muscle fiber was recorded to allow for identification of the corresponding fiber on the serial immunostained section. In this manner, CI and CIV fluorescence quantification and mtDNA analyses were obtained from the same single muscle fibers. Laser microdissection and immunohistochemistry were performed in three batches. One sample was included across all immunohistochemistry batches to calculate a between-batch correction factor for each of the three fluorescence targets of interest (i.e., NDUFB10, MTCO1 and VDAC1).

Mitochondrial DNA copy number and deletion analysis in single muscle fibers

Determination of mtDNA copy number and major arc deletion fraction in microdissected single muscle fibers was performed using a duplex TaqMan quantitative PCR (qPCR) assay. The deletion fraction was determined by comparing a commonly deleted target (*MTND4*) to a rarely deleted target (*MTND1*)[63]. Deletion fractions in muscle samples were normalized to two blood genomic DNA samples from healthy controls, which were included in each experiment to serve as references for non-deleted mtDNA. Absolute quantification was carried out by comparison to a standard series containing PCR-amplified and purified *MTND1* and *MTDN4* templates in known equimolar (10^6, 10^5, 10^4, 10^3, and 10^2 copies/µl). *MTND1* quantity was used to assess mtDNA copy number. For each muscle fiber, mtDNA copy number was calculated per micro dissected area (µm^2). The following primers, probes, and conditions were used: *MTND1* forward primer: 5′-CCCTAAAACCCGCCACATCT-3′, *MTND1* reverse primer: 5′-GAGCGATGGTGAGAGCTAAGGT-3′, *MTND1* MGB probe: 5′-FAM-

CCATCACCCTCTACATCACCGCCC-3′. *MTND4* forward primer: 5′-CCATTCTCCTCCTATCCCTCAAC-3′, *MTND4* reverse primer: 5′-CACAATCTGATGTTTTGGTTAAACTATATTT-3′, *MTND4* MGB probe: 5′-VIC-CCGACATCATTACCGGGTTTTCCTCTTG-3′. For each qPCR reaction, 2 µl of lysate were added to 18 µl of a master mix consisting of primers, probes, and TaqMan Advanced master Mix containing AmpliTaq® Fast DNA Polymerase (ThermoFisher) as per the manufacturer's instruction. Amplification was performed on a StepOnePlus™ Real-Time PCR System (ThermoFisher), using a thermoprofile of one cycle at 95 °C for 20 sec, and 40 cycles at 95 °C for 1 sec and 60 °C for 20 sec. Each sample was run once in triplicate. Data were analyzed from a total of 111 muscle fibers from six individuals with PD and 112 muscle fibers from six controls (14-22 muscle fibers per individual).

Mitochondrial DNA copy number and deletion analysis in bulk muscle tissue

After regressing out the effect of measurement batch, a total of $n = 27$ samples was selected based on CS-normalized CI activity: $n = 8$ PD samples with activity similar to controls, $n = 9$ PD samples with low activity, and $n = 10$ controls samples (Supplementary Fig. 12). These three groups were matched for age (Supplementary Table 1). A transverse section of 20 µm thickness was prepared from each muscle biopsy and collected in a 1.5 mL microtube, and DNA was extracted using the QIAamp® DNA Mini Kit (Qiagen). The resulting extracts were diluted in water to a DNA concentration of 1 ng/mL prior to qPCR. Determination of relative mtDNA copy number and the fraction of major arch deletion was performed in a triplex qPCR targeting *MTND1* and *MTND4*, as well as the nuclear gene *APP*. The following primers, probes, and conditions were used: *MTND1* forward primer: 5′-CCCTAAAACCCGCCACATCT-3′, *MTND1* reverse primer: 5′-GAGCGATGGTGAGAGCTAAGGT-3′, *MTND1* MGB probe: 5′-FAM-CCATCACCCTCTACATCACCGCCC-3′. *MTND4* forward primer: 5′-

572 CCATTCTCCTCCTATCCCTCAAC-3′, *MTND4* reverse primer: 5′-
573 CACAATCTGATGTTTTGGTTAAACTATATTT-3′, *MTND4* MGB probe: 5′-VIC-
574 CCGACATCATTACCGGGTTTTCCTCTTG-3′. *APP* forward primer: 5′-
575 TGTGTGCTCTCCCAGGTCTA-3′, *APP* reverse primer: 5′-CAGTTCTGGATGGTCACTGG
576 -3, *APP* MGB probe: 5′-NED-CCCTGAACTGCAGATCACCAATGTGGTAG-3′. For each
577 qPCR reaction, 2 µl of DNA sample was added to 18 µl of a master mix consisting of primers,
578 probes, and TaqMan Advanced master Mix containing AmpliTaq® Fast DNA Polymerase
579 (ThermoFisher) as per the manufacturer's instruction. Amplification was performed on a
580 StepOnePlus™ Real-Time PCR System (ThermoFisher), using thermal cycling consisting of
581 one cycle at 95 °C for 20 sec, and 40 cycles at 95 °C for 1 sec and 60 °C for 20 sec. Samples
582 were run three times in triplicate. Deletion fraction was determined as described above, while
583 relative mtDNA copy number was calculated from the ratio of *MTND1* to *APP*[64]. A sample
584 from blood genomic DNA was included in each experiment to serve as a non-deleted reference.
585
586 **Mitochondrial DNA sequencing**
587 Sequencing of mtDNA was performed on DNA obtained from both micro-dissected single
588 muscle fibers and bulk muscle tissue. mtDNA was amplified in two overlapping amplicons of
589 9,307 bp (amplicon 1) and 7,814 bp (amplicon 2), corresponding to position 16,330 to 9,068
590 and 8,753 to 16,566 of the Cambridge reference sequence, respectively. The following primers
591 and conditions were used: 9,307 bp amplicon forward primer: 5'-
592 ACATAGCACATTACAGTCAAATCCCTTCTCGTCCC-3', reverse primer: 5'-
593 ATTGCTAGGGTGGCGCTTCCAATTAGGTGC-3', 7,814 bp amplicon forward primer: 5′-
594 TCATTTTTATTGCCACAACTAACCTCCTCGGACTC-3', reverse primer: 5'-
595 CGTGATGTCTTATTTAAGGGGAACGTGTGGGCTAT-3'. For each of the PCR reactions,
596 2 µl of cell lysate was added to 18 µl of a master mix consisting of primers, dNTPs, 5X

PrimeSTAR ® GXL buffer and PrimeSTAR ® GXL (TaKaRa) DNA polymerase, per the manufacturer's instruction. Thermal cycling consisted of one cycle at 92 °C for 2 minutes and 40 cycles at 92 °C for 10 sec, 65 °C for 30 sec and 68 °C for 8 minutes, as well as one final cycle at 68 °C for 8 minutes. Amplification was quality-controlled by gel electrophoresis using 4 µl of the PCR product. Samples with smearing of one or both amplicons were discarded. To establish the heteroplasmic call error introduced by PCR-amplification and DNA sequencing, the same fragments were amplified using a standard reference material mtDNA (Standard Reference Material® 2392-I, NIST, U.S. Department of Commerce) as template. The two amplicons from each sample were pooled prior to shipment to Novogene (UK) Co. Ltd for sequencing using the Illumina platform. The target depth for sequencing was set to 100,000x (~2 Gb per sample). The final mtDNA sequencing dataset consisted of (i) n = 157 single dissected muscle fibers from a total of 12 individuals (77 muscle fibers from 6 individuals with PD and 80 muscle fibers from 6 controls); (ii) one standard reference mtDNA control; (iii) n = 27 bulk muscle tissue samples from a total of 27 individuals (17 individuals with PD and 10 controls). Supplementary Data 1 shows the experimental allocation of subjects. For all samples, raw FASTQ sequencing files were trimmed to exclude low-quality bases and reads using Trimmomatic v0.39[65] with options "ILLUMINACLIP:TruSeq3-PE-2.fa:2:30:10 LEADING:3 TRAILING:3 SLIDINGWINDOW:4:15 MINLEN:36". Raw FASTQ files were assessed using FastQC[66] prior and following trimming. Reads were aligned to the hg38 human genome reference using BWA v0.7.17[67]. Reads mapping to the mitochondrial chromosome were then extracted and duplicates filtered out using GATK MarkDuplicates[68]. To allow for heteroplasmic genotyping, calling of variants was carried out using Mutserve v2.0.0-rc13[69]. To assess potential contamination, we calculated haplotype proportions in each sample using Haplocheck[70], which flagged 2/157 single-fiber samples with >1% contamination (30% and 15%). These fibers were discarded for downstream analyses. Levels of contamination in bulk

622 tissue samples were below 0.6%. Reads with mapping qualities below 20 were removed from
623 the analyses, and calling of heteroplasmy levels were restricted to the revised Cambridge
624 Reference Sequence (rCRS) coordinates 600-8,600 (amplicon 1) and 9,100-16,200 (amplicon
625 2) to ensure adequate depth of coverage and potential sequences originating from the primers.
626 Heteroplasmy levels were only considered if above 1% to ensure at least 10 reads covering the
627 minor allele and restricted to single nucleotide variants (i.e., deletions and insertions were
628 removed). The heteroplasmy level was defined as the heteroplasmy of the minor allele for a
629 given position. The two amplicon regions were analyzed separately since they exhibited
630 different mean depth of coverage.
631
632 **Statistical analyses**
633 *COX/SDH histochemistry data*
634 Due to non-normality of the data, as judged by the Shapiro-Wilk test, the Wilcoxon rank-sum
635 test with continuity correction was used to compare the individual proportions of COX negative
636 or intermediate muscle fibers in the PD and control groups. Pearson's Chi-squared test was used
637 to examine the association between disease state and the group-level proportion of individuals
638 with any COX negative or intermediate muscle fibers. Yate's continuity correction was applied
639 as one expected cell frequency was below 10.
640
641 *Immunohistochemistry fluorescence intensity data*
642 All fluorescence intensity measurements were transformed using base 10 logarithms to improve
643 model fits. To account for mitochondrial content variations, CI level was expressed as the ratio
644 of NDUFB10-fluorescence to VDAC1-fluorescence, and CIV level as the ratio of MTCO1-
645 fluorescence to VDAC1-fluorescence. Throughout the text, CI and CIV levels always refer to
646 their VDAC1-adjusted levels, unless otherwise stated. Kendall rank correlation coefficient was

used to test the correlation between fluorescence intensity data and COX/SDH-status. The correlation between fluorescence measurement in multiple single fibers and in a large section area was assessed by Spearman's Rank Correlation Coefficient, given as $\rho(n-2)$, due to non-normality as judged by the Kolmogorov-Smirnov test. Linear mixed effects regression models were used to compare the PD and control groups. Single muscle fiber VDAC1-fluorescence level, CI level and CIV level were used as the dependent variables, while disease state, age, sex, smoking, and staining batch were included as fixed effects. Additionally, the study subject was added as a random effect to address inter-individual variability. Variance inflation factors (VIF) did not indicate collinearity. The analyses were repeated in a dataset consisting of one large section area measurement per individual, using linear regression models with the same independent variables.

Enzyme activity data

To account for differences in mitochondrial content, the complex activities were normalized to the activity of citrate synthase. The resulting normalized activity measures (CI-CIV/CS), as well as CS activity alone, were log transformed using base 10 logarithms to improve model fits and used as dependent variables in linear regression models. The models included disease state, age, sex, and measurement batch as independent variables. Analyses were repeated, adding smokers and including smoking as an additional variable. Variance inflation factors (VIF) did not indicate collinearity. The comparisons of the PD and control groups for the four complexes were corrected for multiplicity using the Benjamini-Hochberg procedure. The analysis of CI/CS was also performed separately in the PD group, with MDS-UPDRS III score, MoCA score, disease duration, age, sex and measurement batch as independent variables.

Comparisons between the PD subgroups with low and control-like CI/CS activity were conducted by Student's *t*-test for MoCA scores and age of onset, since the Shapiro-Wilk test indicated normality and the F-test indicated equality of variance. Wilcoxon rank-sum test with continuity correction was used to compare MDS-UPDRS III scores due to non-normality. The Fisher's exact test was used to test the association between CI/CS subgroup and motor phenotype (tremor dominant, postural instability/gait difficulty) and sex. These analyses were corrected for multiplicity using the Benjamini-Hochberg procedure.

Adjustment of immunohistochemistry data and enzymatic activity data for batch effects

For visualization and selected analyses, immunohistochemistry fluorescence intensity data and enzymatic activity data were adjusted for the effects of batch. For the fluorescence intensity data (e.g., CI level), linear regression models were fitted using only staining batch as the independent variable. Similarly, for the enzymatic activity data (e.g., CI/CS), models were fitted using only measurement batch as the independent variable. In all instances, the dependent variable was log transformed using base 10 logarithms to improve model fits. The residuals from these regressions (i.e., variation in the data not explained by batch) were extracted and the intercept of the regression was re-added to maintain the original scale. The resulting batch adjusted data were used when plotting the distribution of fluorescence intensity data and enzymatic activity data; for calculating Cohen's *d* for the difference in CI/CS activity between the PD and control group; for the classification of the PD subgroups with low and control-like CI/CS activity; to assess the association between CI/CS activity and CI quantity; and for the selection of samples for mtDNA analysis in single fibers and bulk tissue.

Association between complex I enzyme activity data and immunohistochemistry data

The association between CI activity and quantity was assessed a linear regression model with CI/CS as dependent variable, and disease state, age, sex and CI level (NDUFB10/VDAC1) as independent variables, using fluorescence measurements from large section areas. Batch adjusted data was used, and both CI/CS activity data and CI level data were transformed using base 10 logarithms. To assess whether including CI level data significantly improved model fit, an analysis of variance (ANOVA) was conducted using the *anova* function in R to compare the model with and without CI level as a covariate.

mtDNA data

Single fiber mtDNA copy number and major arc deletion fraction were assessed in linear mixed effects regression models that included disease state, age, sex, and qPCR plate as fixed effects. The study subject was added as a random effect variable to account for inter-individual variability. Variance inflation factors (VIF) did not indicate collinearity. Due to non-normality of the data as judged by the Kolmogorov-Smirnov test and the Shapiro-Wilk test, the correlations between mtDNA parameters and immunohistochemical fluorescence intensity measurements were assessed by Spearman's Rank Correlation Coefficient, given as $\rho(n-2)$. In bulk muscle tissue, due to non-normality of the data as judged by the Shapiro-Wilk test, the Wilcoxon rank sum test with continuity correction was used to compare mtDNA copy number and deletion fraction between the PD group with CI activity similar to controls and the PD group with low CI activity, as well as between each PD group and the control group. For single fibers, the heteroplasmic load was modelled as the sum of the heteroplasmic levels (above 1 %) across the entire amplicon region as a function of disease state, age, sex, and single fiber CI level, accounting for individual as a random effect using linear mixed effects model. For bulk muscle tissue samples, the same measure of heteroplasmic load was employed (i.e. the sum of the heteroplasmic levels). To assess the association between heteroplasmic load and disease

720 status (i.e., PD-normal CI activity, PD-low CI activity, and control) the Kruskal-Wallis test was
721 used, due to non-normality of the data as assessed by the Kolmogorov-Smirnov test. The
722 association between heteroplasmic load and CI activity was then assessed, with a linear
723 regression model with log(CI/CS) as the independent variable and accounting for activity
724 measurement batch.
725
726 All analyses were performed using R version 4.3.0 (R Core Team, 2023) in RStudio 2023.03.1
727 Build 446 (2009-2023 Posit Software, PBC). Linear mixed effects regression models were done
728 using the *lme4* package V1.1.35.1[71]. The *ggplot2* package V3.4.4 was used for plots[72].
729 Adjusting data for the effect of batch, as described above, was achieved using the *adjust*
730 function of the *datawizard* package V0.9.1.[73]
731

732 ## Code availability statement

733 The immunohistochemistry, enzymatic activity and mtDNA qPCR data generated in this study
734 are provided in the Supplementary Data files. The sequencing data of the bulk tissue samples
735 and the single muscle fiber samples will be available in the Federated European Genome-
736 phenome Archive (FEGA) Norway. FEGA Accession codes will be available shortly and before
737 publication. The code required to reproduce the results of the statistical analyses are available
738 in GitLab: https://git.app.uib.no/simon.kverneng/complex-i-deficiency-in-skeletal-muscle-of-
739 a-subgroup-of-parkinsons-disease.

References

1. Postuma, R. B. *et al.* MDS clinical diagnostic criteria for Parkinson's disease: MDS-PD Clinical Diagnostic Criteria. *Mov. Disord.* **30**, 1591–1601 (2015).
2. de Rijk, M. C. *et al.* Prevalence of Parkinson's disease in Europe: A collaborative study of population-based cohorts. Neurologic Diseases in the Elderly Research Group. *Neurology* **54**, S21-3 (2000).
3. Gooch, C. L., Pracht, E. & Borenstein, A. R. The burden of neurological disease in the United States: A summary report and call to action. *Ann Neurol* **81**, 479–484 (2017).
4. Dorsey, E. R. *et al.* Global, regional, and national burden of Parkinson's disease, 1990–2016: a systematic analysis for the Global Burden of Disease Study 2016. *Lancet Neurol.* **17**, 939–953 (2018).
5. Athauda, D. & Foltynie, T. The ongoing pursuit of neuroprotective therapies in Parkinson disease. *Nat. Rev. Neurol.* **11**, 25–40 (2015).
6. Espay, A. J. *et al.* Biomarker-driven phenotyping in Parkinson disease: a translational missing link in disease-modifying clinical trials. *Mov. Disord. Off. J. Mov. Disord. Soc.* **32**, 319–324 (2017).
7. Greenland, J. C., Williams-Gray, C. H. & Barker, R. A. The clinical heterogeneity of Parkinson's disease and its therapeutic implications. *Eur J Neurosci* **49**, 328–338 (2019).
8. Chen-Plotkin, A. S. *et al.* Finding Useful Biomarkers for Parkinson's Disease. *Sci. Transl. Med.* **10**, (2018).
9. Halliday, G. M. & McCann, H. The progression of pathology in Parkinson's disease. *Ann. N. Y. Acad. Sci.* **1184**, 188–195 (2010).
10. Espay, A. J. *et al.* Biomarker-driven phenotyping in Parkinson's disease: A translational missing link in disease-modifying clinical trials. *Mov. Disord.* **32**, 319–324 (2017).

11. Lawton, M. *et al.* Developing and validating Parkinson's disease subtypes and their motor and cognitive progression. *J. Neurol. Neurosurg. Psychiatry* **89**, 1279–1287 (2018).
12. Lawton, M. *et al.* Parkinson's Disease Subtypes in the Oxford Parkinson Disease Centre (OPDC) Discovery Cohort. *J. Park. Dis.* **5**, 269–279 (2015).
13. Grünewald, A., Kumar, K. R. & Sue, C. M. New insights into the complex role of mitochondria in Parkinson's disease. *Prog. Neurobiol.* **177**, 73–93 (2019).
14. Schapira, A. H. *et al.* Mitochondrial complex I deficiency in Parkinson's disease. *Lancet* **1**, 1269 (1989).
15. Flønes, I. H. & Tzoulis, C. Mitochondrial Respiratory Chain Dysfunction—A Hallmark Pathology of Idiopathic Parkinson's Disease? *Front. Cell Dev. Biol.* **10**, 874596 (2022).
16. Subrahmanian, N. & LaVoie, M. J. Is there a special relationship between complex I activity and nigral neuronal loss in Parkinson's disease? A critical reappraisal. *Brain Res.* **1767**, 147434 (2021).
17. Flønes, I. H. *et al.* Mitochondrial complex I deficiency stratifies idiopathic Parkinson's disease. *Nat. Commun.* **15**, 3631 (2024).
18. Lawless, C., Greaves, L., Reeve, A. K., Turnbull, D. M. & Vincent, A. E. The rise and rise of mitochondrial DNA mutations. *Open Biol.* **10**, 200061 (2020).
19. Murphy, J. L. *et al.* Cytochrome c oxidase-intermediate fibres: Importance in understanding the pathogenesis and treatment of mitochondrial myopathy. *Neuromuscul. Disord.* **22**, 690–698 (2012).
20. Fetterman, J. L., Sammy, M. J. & Ballinger, S. W. Mitochondrial toxicity of tobacco smoke and air pollution. *Toxicology* **391**, 18–33 (2017).
21. Smith, P. R., Cooper, J. M., Govan, G. G., Harding, A. E. & Schapira, A. H. Smoking and mitochondrial function: a model for environmental toxins. *Q. J. Med.* **86**, 657–660 (1993).

788 22. van der Toorn, M. *et al.* Cigarette smoke-induced blockade of the mitochondrial
789 respiratory chain switches lung epithelial cell apoptosis into necrosis. *Am. J. Physiol.*
790 *Lung Cell. Mol. Physiol.* **292**, L1211-1218 (2007).
791 23. Decker, S. T., Alexandrou-Majaj, N. & Layec, G. Effects of acute cigarette smoke
792 concentrate exposure on mitochondrial energy transfer in fast- and slow-twitch skeletal
793 muscle. *Biochim. Biophys. Acta Bioenerg.* **1864**, 148973 (2023).
794 24. Cormier, A., Morin, C., Zini, R., Tillement, J. P. & Lagrue, G. In vitro effects of nicotine
795 on mitochondrial respiration and superoxide anion generation. *Brain Res.* **900**, 72–79
796 (2001).
797 25. Shoffner, J. M., Watts, R. L., Juncos, J. L., Torroni, A. & Wallace, D. C. Mitochondrial
798 oxidative phosphorylation defects in Parkinson's disease. *Ann. Neurol.* **30**, 332–339
799 (1991).
800 26. Cardellach, F. *et al.* Mitochondrial respiratory chain activity in skeletal muscle from
801 patients with Parkinson's disease. *Neurology* **43**, 2258–2262 (1993).
802 27. Winkler-Stuck, K. *et al.* Re-evaluation of the dysfunction of mitochondrial respiratory
803 chain in skeletal muscle of patients with Parkinson?s disease. *J. Neural Transm.* **112**,
804 499–518 (2005).
805 28. Penn, A. M. *et al.* Generalized mitochondrial dysfunction in Parkinson's disease detected
806 by magnetic resonance spectroscopy of muscle. *Neurology* **45**, 2097–2099 (1995).
807 29. Mischley, L. K. *et al.* ATP and NAD+ Deficiency in Parkinson's Disease. *Nutrients* **15**,
808 943 (2023).
809 30. Krige, D., Carroll, M. T., Cooper, J. M., Marsden, C. D. & Schapira, A. H. Platelet
810 mitochondrial function in Parkinson's disease. The Royal Kings and Queens Parkinson
811 Disease Research Group. *Ann. Neurol.* **32**, 782–788 (1992).

812 31. Yoshino, H., Nakagawa-Hattori, Y., Kondo, T. & Mizuno, Y. Mitochondrial complex I
813 and II activities of lymphocytes and platelets in Parkinson's disease. *J. Neural Transm. Park. Dis. Dement. Sect.* **4**, 27–34 (1992).
815 32. Gu, M., Cooper, J. M., Taanman, J. W. & Schapira, A. H. Mitochondrial DNA
816 transmission of the mitochondrial defect in Parkinson's disease. *Ann. Neurol.* **44**, 177–186
817 (1998).
818 33. Benecke, R., Strümper, P. & Weiss, H. Electron transfer complexes I and IV of platelets
819 are abnormal in Parkinson's disease but normal in Parkinson-plus syndromes. *Brain J. Neurol.* **116 (Pt 6)**, 1451–1463 (1993).
821 34. Haas, R. H. *et al.* Low platelet mitochondrial complex I and complex II/III activity in
822 early untreated Parkinson's disease. *Ann. Neurol.* **37**, 714–722 (1995).
823 35. Carling, P. J. *et al.* Deep phenotyping of peripheral tissue facilitates mechanistic disease
824 stratification in sporadic Parkinson's disease. *Prog. Neurobiol.* **187**, 101772 (2020).
825 36. Milanese, C. *et al.* Peripheral mitochondrial function correlates with clinical severity in
826 idiopathic Parkinson's disease. *Mov. Disord. Off. J. Mov. Disord. Soc.* **34**, 1192–1202
827 (2019).
828 37. Winkler-Stuck, K., Wiedemann, F. R., Wallesch, C.-W. & Kunz, W. S. Effect of
829 coenzyme Q10 on the mitochondrial function of skin fibroblasts from Parkinson patients.
830 *J. Neurol. Sci.* **220**, 41–48 (2004).
831 38. Barroso, N. *et al.* Respiratory chain enzyme activities in lymphocytes from untreated
832 patients with Parkinson disease. *Clin. Chem.* **39**, 667–669 (1993).
833 39. Müftüoglu, M. *et al.* Mitochondrial complex I and IV activities in leukocytes from
834 patients with parkin mutations. *Mov. Disord.* **19**, 544–548 (2004).
835 40. Shults, C. W. *et al.* Carbidopa/levodopa and selegiline do not affect platelet mitochondrial
836 function in early parkinsonism. *Neurology* **45**, 344–348 (1995).

837 41. Dagani, F., Ferrari, R., Anderson, J. J. & Chase, T. N. L-dopa does not affect electron
838 transfer chain enzymes and respiration of rat muscle mitochondria. *Mov. Disord. Off. J.*
839 *Mov. Disord. Soc.* **6**, 315–319 (1991).
840 42. Fløthings, I. H. *et al.* Neuronal complex I deficiency occurs throughout the Parkinson's
841 disease brain, but is not associated with neurodegeneration or mitochondrial DNA
842 damage. *Acta Neuropathol. (Berl.)* **135**, 409–425 (2018).
843 43. Nalls, M. A. *et al.* Identification of novel risk loci, causal insights, and heritable risk for
844 Parkinson's disease: a meta-analysis of genome-wide association studies. *Lancet Neurol.*
845 **18**, 1091–1102 (2019).
846 44. Gaare, J. J. *et al.* Rare genetic variation in mitochondrial pathways influences the risk for
847 Parkinson's disease: Mitochondrial Pathways In PD. *Mov. Disord.* **33**, 1591–1600 (2018).
848 45. Robak, L. A. *et al.* Excessive burden of lysosomal storage disorder gene variants in
849 Parkinson's disease. *Brain* **140**, 3191–3203 (2017).
850 46. Arena, G. *et al.* Polygenic Risk Scores Validated in Patient-Derived Cells Stratify for
851 Mitochondrial Subtypes of Parkinson's Disease. *Ann. Neurol.* **n/a**,.
852 47. Degli Esposti, M. Inhibitors of NADH–ubiquinone reductase: an overview. *Biochim.*
853 *Biophys. Acta BBA - Bioenerg.* **1364**, 222–235 (1998).
854 48. Tanner, C. M. *et al.* Rotenone, paraquat, and Parkinson's disease. *Environ. Health*
855 *Perspect.* **119**, 866–872 (2011).
856 49. Richardson, J. R., Fitsanakis, V., Westerink, R. H. S. & Kanthasamy, A. G. Neurotoxicity
857 of pesticides. *Acta Neuropathol. (Berl.)* **138**, 343–362 (2019).
858 50. Zirra, A. *et al.* Gender Differences in the Prevalence of Parkinson's Disease. *Mov. Disord.*
859 *Clin. Pract.* **10**, 86–93 (2023).

860 51. Fernandez-Vizarra, E. & Zeviani, M. Blue-Native Electrophoresis to Study the OXPHOS
861 Complexes. in *Mitochondrial Gene Expression* (eds. Minczuk, M. & Rorbach, J.) vol.
862 2192 287–311 (Springer US, New York, NY, 2021).
863 52. Cabrera-Orefice, A., Potter, A., Evers, F., Hevler, J. F. & Guerrero-Castillo, S.
864 Complexome Profiling—Exploring Mitochondrial Protein Complexes in Health and
865 Disease. *Front. Cell Dev. Biol.* **9**, 796128 (2022).
866 53. Gaare, J. J., Skeie, G. O., Tzoulis, C., Larsen, J. P. & Tysnes, O.-B. Familial aggregation
867 of Parkinson's disease may affect progression of motor symptoms and dementia. *Mov.*
868 *Disord. Off. J. Mov. Disord. Soc.* **32**, 241–245 (2017).
869 54. Lunde, K. A. *et al.* Association of glucocerebrosidase polymorphisms and mutations with
870 dementia in incident Parkinson's disease. *Alzheimers Dement. J. Alzheimers Assoc.* **14**,
871 1293–1301 (2018).
872 55. Stige, K. E. *et al.* The STRAT-PARK cohort: a personalized initiative to stratify
873 Parkinson's disease. *Prog. Neurobiol.* 102603 (2024)
874 doi:10.1016/j.pneurobio.2024.102603.
875 56. Brakedal, B. *et al.* The NADPARK study: A randomized phase I trial of nicotinamide
876 riboside supplementation in Parkinson's disease. *Cell Metab.* **34**, 396-407.e6 (2022).
877 57. Goetz, C. G. *et al.* Movement Disorder Society-sponsored revision of the Unified
878 Parkinson's Disease Rating Scale (MDS-UPDRS): scale presentation and clinimetric
879 testing results. *Mov. Disord. Off. J. Mov. Disord. Soc.* **23**, 2129–2170 (2008).
880 58. Stebbins, G. T. *et al.* How to identify tremor dominant and postural instability/gait
881 difficulty groups with the movement disorder society unified Parkinson's disease rating
882 scale: Comparison with the unified Parkinson's disease rating scale: PIGD and The MDS-
883 UPDRS. *Mov. Disord.* **28**, 668–670 (2013).

884 59. Nasreddine, Z. S. *et al.* The Montreal Cognitive Assessment, MoCA: A Brief Screening
885 Tool For Mild Cognitive Impairment. *J. Am. Geriatr. Soc.* **53**, 695–699 (2005).
886 60. Rocha, M. C. *et al.* A novel immunofluorescent assay to investigate oxidative
887 phosphorylation deficiency in mitochondrial myopathy: understanding mechanisms and
888 improving diagnosis. *Sci. Rep.* **5**, 15037 (2015).
889 61. Old, S. L. & Johnson, M. A. Methods of microphotometric assay of succinate
890 dehydrogenase and cytochromec oxidase activities for use on human skeletal muscle.
891 *Histochem. J.* **21**, 545–555 (1989).
892 62. Brischigliaro, M., Frigo, E., Fernandez-Vizarra, E., Bernardi, P. & Viscomi, C.
893 Measurement of mitochondrial respiratory chain enzymatic activities in Drosophila
894 melanogaster samples. *STAR Protoc.* **3**, 101322 (2022).
895 63. Dölle, C. *et al.* Defective mitochondrial DNA homeostasis in the substantia nigra in
896 Parkinson disease. *Nat. Commun.* **7**, 13548 (2016).
897 64. Tzoulis, C. *et al.* Severe nigrostriatal degeneration without clinical parkinsonism in
898 patients with polymerase gamma mutations. *Brain* **136**, 2393–2404 (2013).
899 65. Bolger, A. M., Lohse, M. & Usadel, B. Trimmomatic: a flexible trimmer for Illumina
900 sequence data. *Bioinforma. Oxf. Engl.* **30**, 2114–2120 (2014).
901 66. Andrews, S. Babraham Bioinformatics - FastQC A Quality Control tool for High
902 Throughput Sequence Data. https://www.bioinformatics.babraham.ac.uk/projects/fastqc/
903 (2010).
904 67. Li, H. & Durbin, R. Fast and accurate short read alignment with Burrows-Wheeler
905 transform. *Bioinforma. Oxf. Engl.* **25**, 1754–1760 (2009).
906 68. Auwera, G. van der & O'Connor, B. D. *Genomics in the Cloud: Using Docker, GATK,*
907 *and WDL in Terra*. (O'Reilly Media, Sebastopol, CA, 2020).

908 69. Weissensteiner, H. *et al.* mtDNA-Server: next-generation sequencing data analysis of
909 human mitochondrial DNA in the cloud. *Nucleic Acids Res.* **44**, W64-69 (2016).
910 70. Weissensteiner, H. *et al.* Contamination detection in sequencing studies using the
911 mitochondrial phylogeny. *Genome Res.* **31**, 309–316 (2021).
912 71. Bates, D., Mächler, M., Bolker, B. & Walker, S. Fitting Linear Mixed-Effects Models
913 Using **lme4**. *J. Stat. Softw.* **67**, (2015).
914 72. Wickham, H. *et al.* ggplot2: Create Elegant Data Visualisations Using the Grammar of
915 Graphics. (2024).
916 73. Patil, I. *et al.* datawizard: An R Package for Easy Data Preparation andStatistical
917 Transformations. *J. Open Source Softw.* **7**, 4684 (2022).

Acknowledgements

We are grateful to the study participants and their families for their essential contribution to the study. We thank the STRAT-PARK study teams at Haukeland University Hospital and St. Olav's University Hospital, including research nurses Erika Sheard, Mona Søgnen, Solveig Af Geijerstam, Therese Vetås, and Anne Grete Wahlvåg, as well as laboratory personnel Martina Castelli, Yana Mikhaleva, Gry Hilde Nilsen, Omnia Shadad, Dagny Ann Sandnes, and Ida Johansson for the outstanding technical support. We are also grateful to the STRAT-COG study team, including Kristina Skeie and Lone Birkeland Johnsen, and the NADPARK study team, including research nurse Marit Renså. We thank Nelson Osuagwu for technical assistance with fluorescence image acquisition. The fluorescence imaging was performed at the Molecular Imaging Center, Dept. of Biomedicine, University of Bergen. This work is supported by grants from The Michel J Fox Foundation (MJFF-022567, CT), The Research Council of Norway (288164; CT), The KG Jebsen Foundation (SKGJ-MED-023; CT), and the Western Norway Regional Health Authority (F-12598-D12092; SK).

Author contributions

S.U.K.: participated in study conception and design, led the study, recruited and assessed study participants, collected, analyzed and interpreted data, and drafted the manuscript. K.E.S.: participated in study conception and design, recruited and assessed study participants, collected and interpreted data. H.B., K.L., B.B., G.O.S., R.E.S., K.H.: recruited and assessed study participants, collected and interpreted data. S.M., M.B., E.F.V: collected and interpreted data and participated in the drafting of the manuscript. I.F.: participated in data collection and interpretation. L.T.: participated in study design and advised on statistical approaches. Y.N.T.C.: participated in study conception and funding acquisition. C.D.: participated in study conception, design, data interpretation and data collection. G.S.N.: generated, analyzed and

943 interpreted data and drafted the manuscript. C.T.: conceived, designed and directed the study,
944 contributed to data analyses and interpretation, drafted the manuscript, and acquired funding
945 for the study. All authors have read and approved the manuscript.

946

947 ## Competing interests

948 The authors declare no competing interests.

949

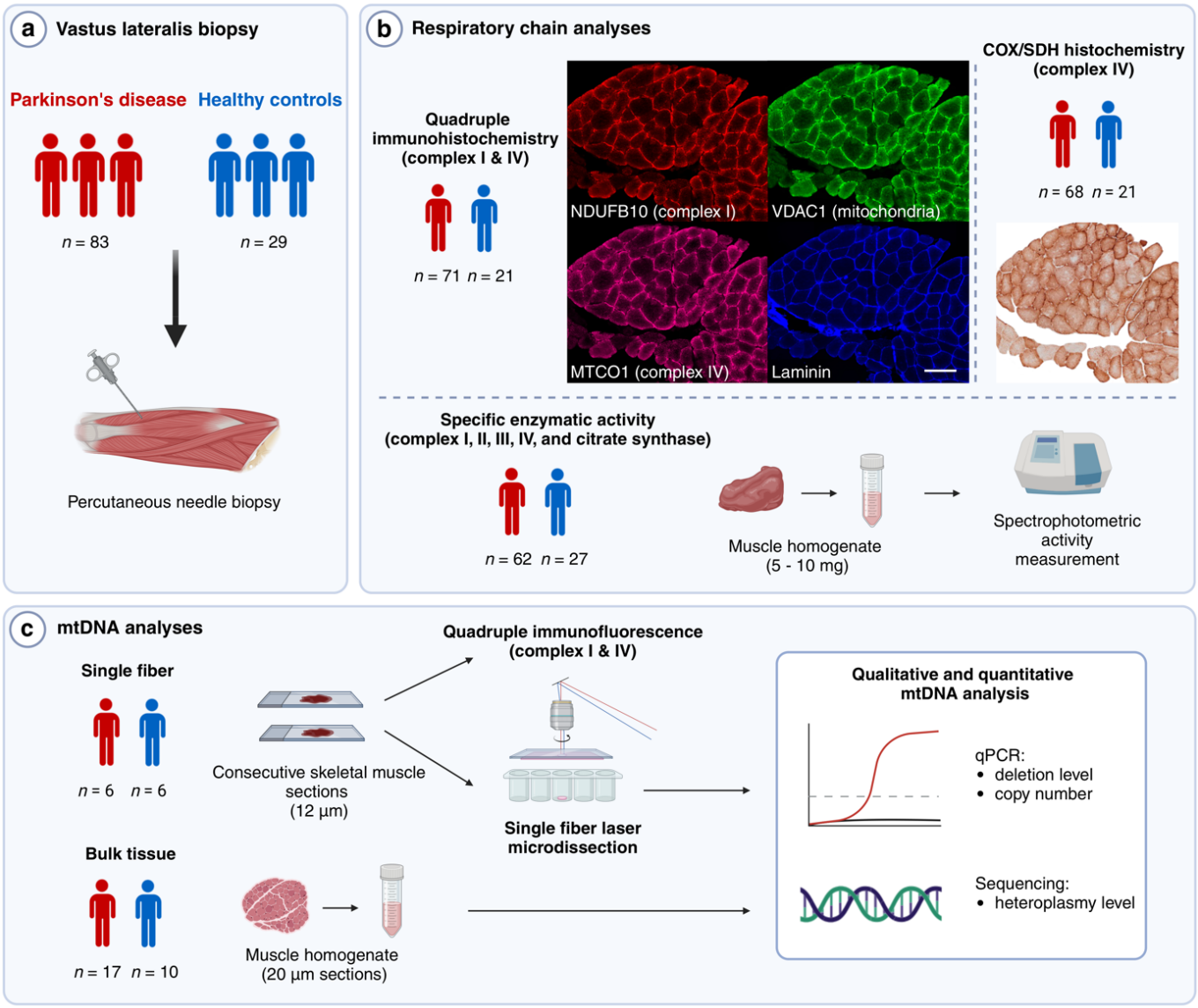

950

951 **Figure 1. Assessment of mitochondrial respiratory chain integrity in skeletal muscle**
952 **biopsies from individuals with PD and neurologically healthy controls.**

953 **(a)** Needle biopsies of the vastus lateralis muscle were collected from individuals with PD and
954 neurologically healthy controls. **(b)** Respiratory chain analyses: Quadruple
955 immunohistochemistry was used for quantitative analysis of complexes I and IV (CI and CIV),
956 the mitochondrial mass marker VDAC1, and for identifying single muscle fibers by laminin
957 staining. Scale bar: 200 µm. Cytochrome c oxidase/succinate dehydrogenase (COX/SDH)
958 histochemistry and spectrophotometric mitochondrial respiratory chain (MRC) complex
959 activity assays were used for functional analysis of complexes I-IV (CI-IV) and citrate synthase

(CS). **(c)** mtDNA analyses: The association between the quantity and function of CI and qualitative or quantitative changes in mtDNA was assessed. A subset of PD and control samples were selected for analysis. mtDNA copy number and deletions were assessed by quantitative PCR, and point variations were examined by PCR amplification and ultra-deep DNA sequencing, in both bulk muscle tissue and single muscle fibers. Figure created with BioRender.com

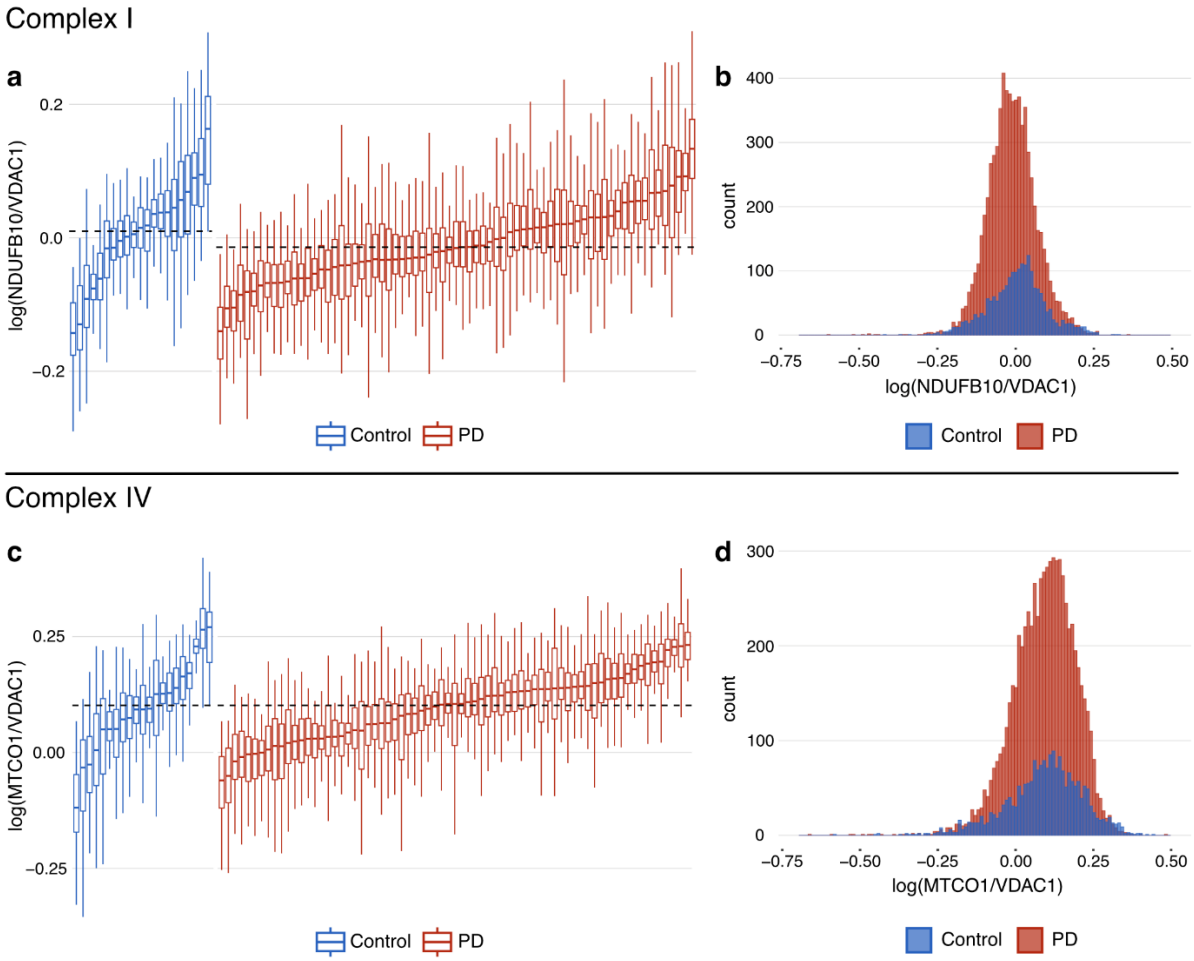

966

967 **Figure 2. Immunohistochemistry shows no quantitative changes of complexes I or IV in**

968 **PD single muscle fibers.**

969 Complex I (NDUFB10) and complex IV (MTCO1) fluorescence intensity normalized to

970 mitochondrial mass (VDAC1) in single muscle fibers (*n* = 75-100 per individual) in the PD

971 (red) and control (blue) groups. Values are log transformed. For the purpose of visualization,

972 the data have been adjusted for the effect of staining batch by regressing out this variable (see

973 Methods section). Boxplots **(a, c)** show individual-level distributions of single fiber

974 measurement where each box represents one individual. Boxes: median and interquartile range

975 (IQR); whiskers: 1.5 x IQR from the lower and upper quartiles. Individuals are sorted by median

976 values from left to right. Dashed lines show the group-level medians of the PD and control

977 groups. The histograms **(b, d)** represent group-level distributions of single fiber measurement

978 in the PD and control groups. Supplementary Fig. 5 shows the same data without adjusting for
979 batch.

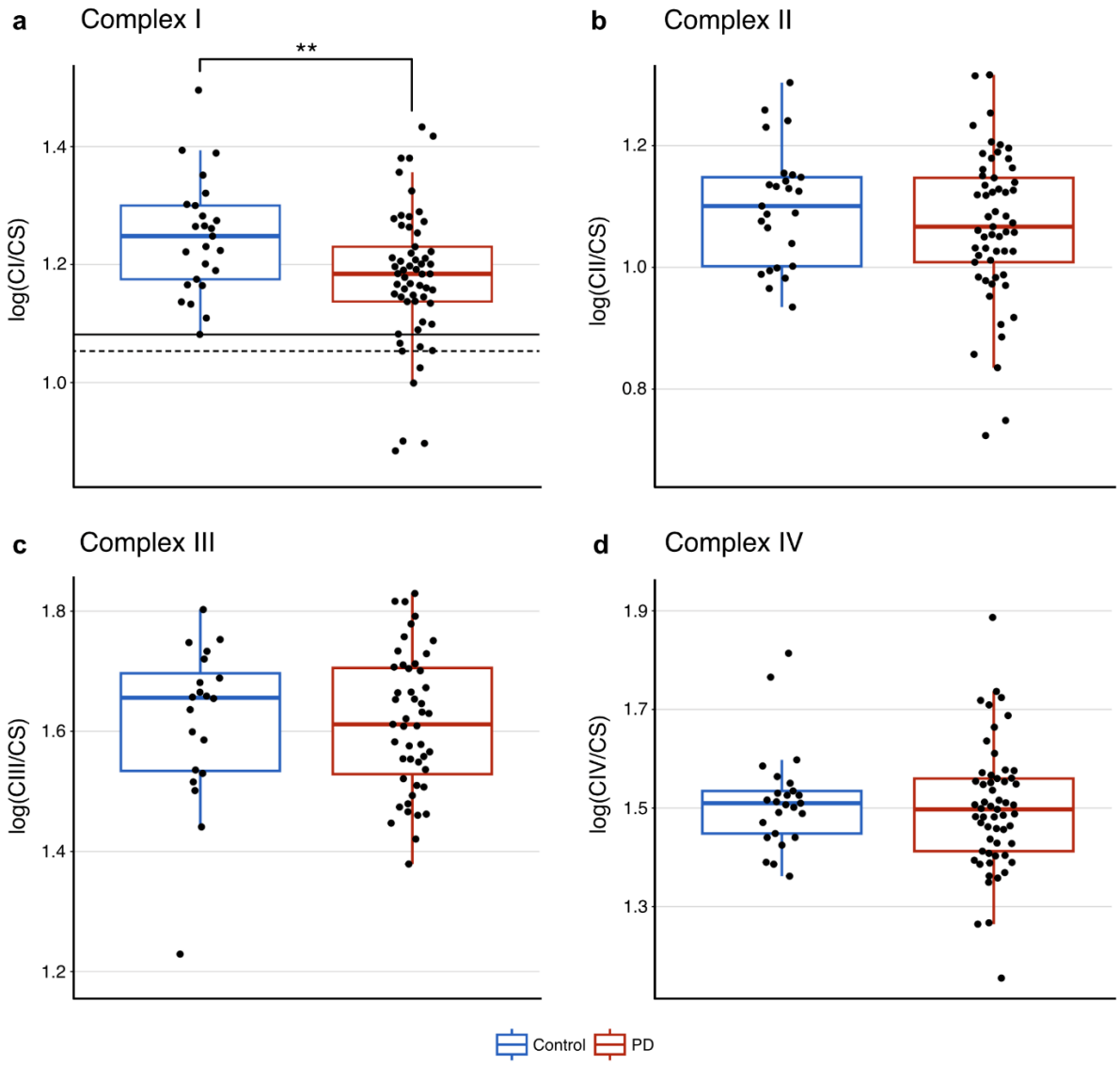

Figure 3. Spectrophotometric activity measurement in muscle shows lower complex I activity in PD.

Activities of complexes I-IV (CI-IV), normalized to citrate synthase (CS) activity are shown. Values are log transformed. For the purpose of visualization, the data have been adjusted for the effect of measurement batch by regressing out this variable (see Methods section). Smokers have been removed from the dataset (Supplementary Fig. 7-9 show the same data without adjusting for batch effects and including active smokers). Red boxplots represent the PD group and blue boxplots represent the control group. Boxes: median and interquartile range (IQR); whiskers: 1.5 x IQR from the lower and upper quartiles. Individuals are sorted by median values

991 from left to right. Each dot represents one individual. **(a)** CS-normalized CI activity. The solid
992 line indicates the lower end of the control distribution. The dotted line indicates minus 2
993 standard deviations from the mean of controls. **(b)** CS-normalized CII activity. **(c)** CS-
994 normalized CIII activity. Measurements from 15 samples were excluded from this analysis due
995 to technical issues with the reduction of decylubiquinone (Supplementary Data 1). **(d)** CS-
996 normalized CIV activity.

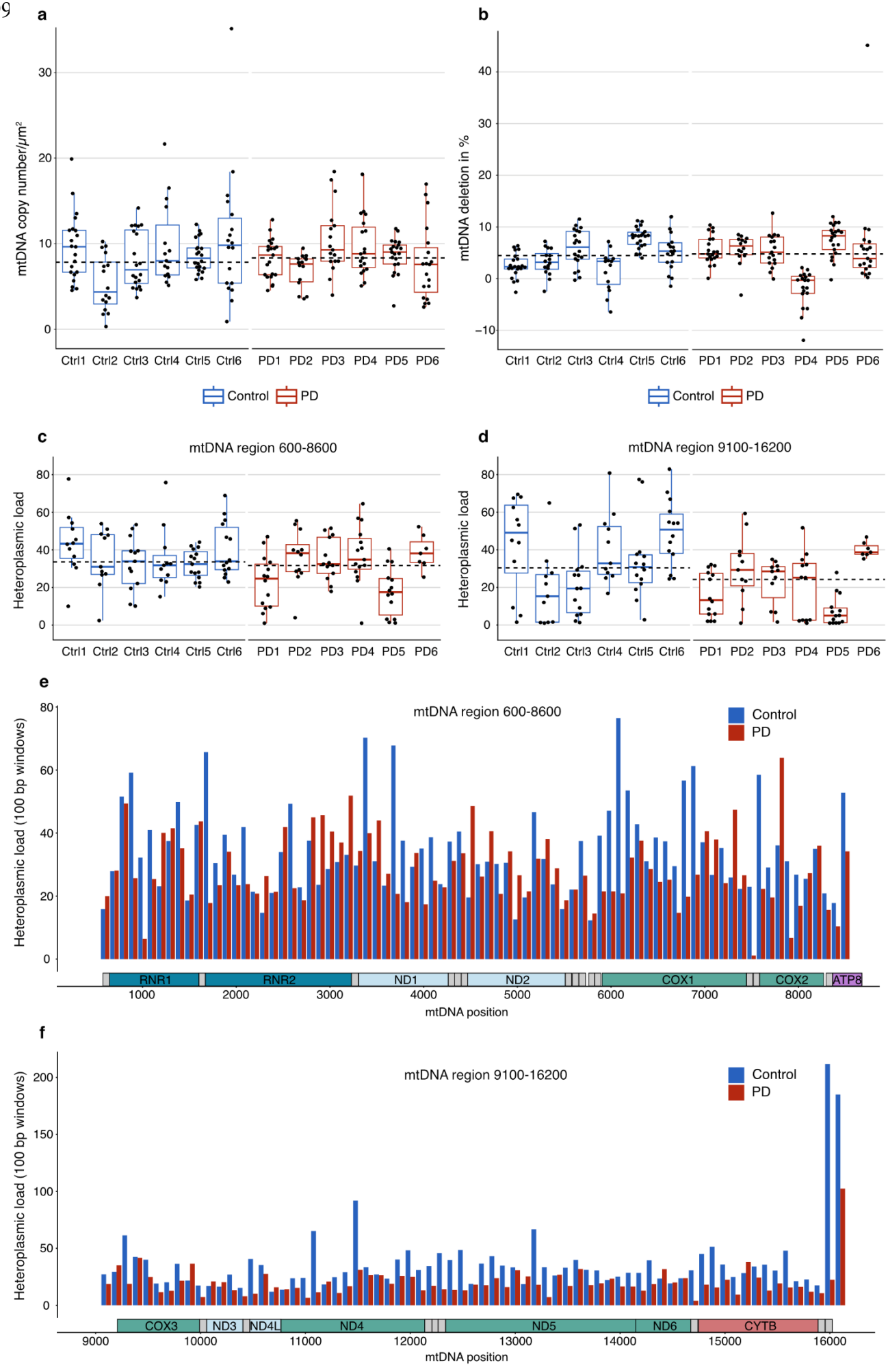

Figure 4. Single muscle fiber mitochondrial DNA profile shows no difference between PD and control muscle.

Single muscle fiber mitochondrial DNA (mtDNA) profile from six individuals with PD and six controls. mtDNA copy number and major arc deletion fraction were assessed in a total of 223 muscle fibers, and 157 of the same fibers were analyzed for sequence variation. Red boxplots represent individuals with PD and blue boxplots represent controls. Boxes: median and interquartile range (IQR); whiskers: 1.5 x IQR from the lower and upper quartiles. Individuals are sorted by median values from left to right. Each dot represents a single muscle fiber. Dashed lines show group-level medians. **(a)** mtDNA copy number per micro dissected area (μm^2) in single muscle fibers (n = 14-22 per individual). **(b)** Major arc deletion fractions in the same muscle fibers. Deletion fractions were calculated in reference to two samples from blood genomic DNA from healthy controls, which were defined as non-deleted. **(c-d)** Heteroplasmic load in single muscle fibers, defined as the sum of the heteroplasmy values across the mtDNA region, assessed separately in the regions 600-8600 (amplicon 1) and 9100-16200 (amplicon 2). Heteroplasmy levels were only considered if above 1% and restricted to single nucleotide variants. **(e-f)** The distribution of heteroplasmy within the mtDNA in the PD (red) and control (blue) groups is shown as the sum of all heteroplasmic levels in 100 bp windows (y-axis) across the mtDNA amplicons (mtDNA coordinates, x-axis).

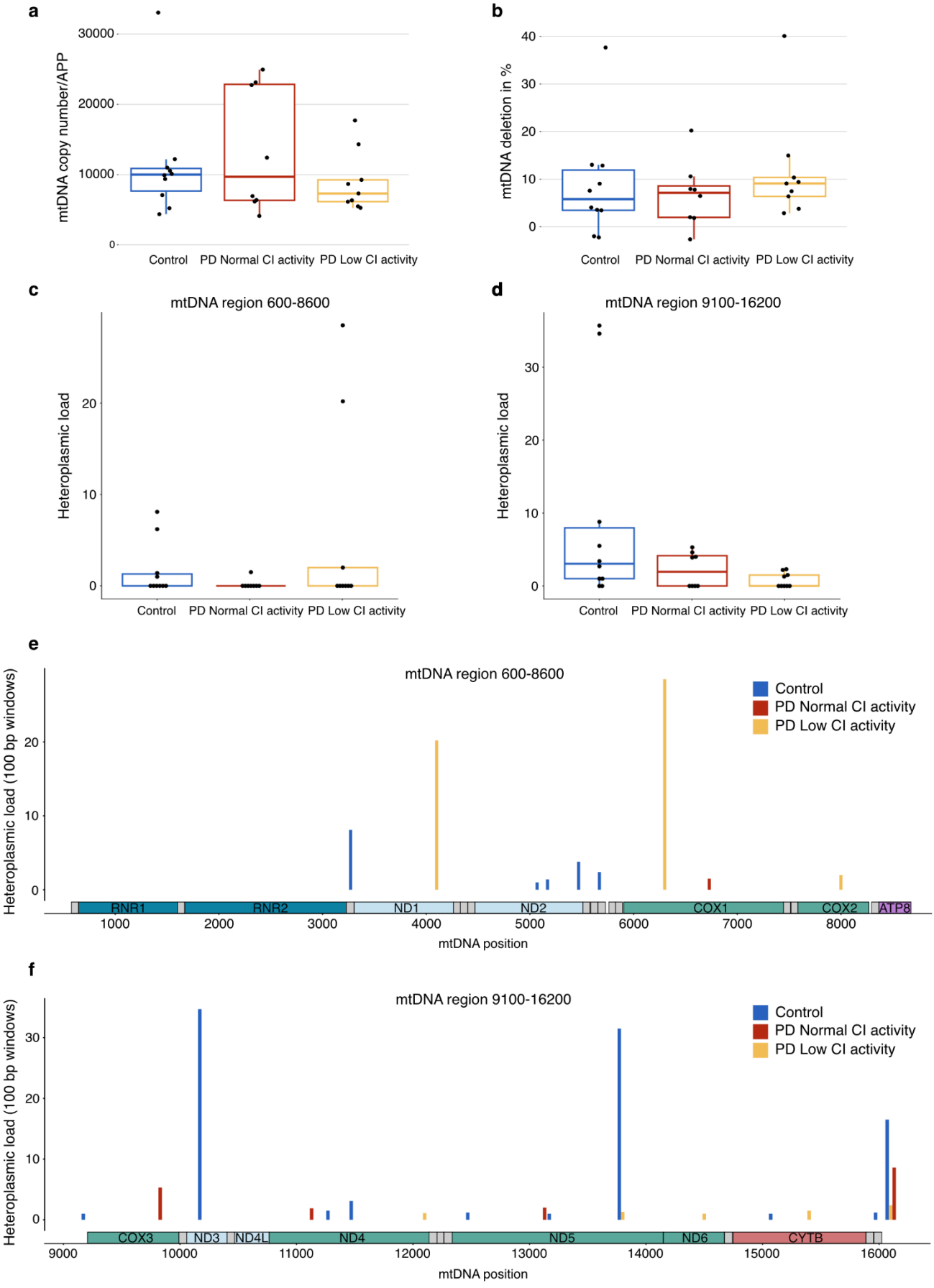

1016

Figure 5. Functional complex I deficiency in PD muscle is not associated with mitochondrial DNA changes.

Bulk muscle tissue mitochondrial DNA (mtDNA) analyses from 8 PD individuals with complex I (CI) activity similar to controls (red boxplots and bars), 9 PD individuals with low CI activity (yellow boxplots and bars), and 10 controls (blue boxplot and bars). The groups were matched for age. Boxes: median and interquartile range (IQR); whiskers: 1.5 x IQR from the lower and upper quartiles. Individuals are sorted by median values from left to right. Each dot represents one individual. **(a)** mtDNA copy number in bulk muscle tissue, normalized to the nuclear gene *APP*. **(b)** Major arc deletion fractions in bulk muscle tissue. **(c-d)** Heteroplasmic load in bulk muscle tissue, defined as the sum of the heteroplasmy values across the mtDNA region, assessed separately in the regions 600-8600 (amplicon 1) and 9100-16200 (amplicon 2). Heteroplasmy levels were only considered if above 1% and restricted to single nucleotide variants. **(e-f)** The distribution of heteroplasmy within the mtDNA in the three groups is shown as the sum of all heteroplasmic levels in 100 bp windows (y-axis) across the mtDNA amplicons (mtDNA coordinates, x-axis).

Table 1: Demographic and clinical characteristics

	Group	
Variable	**PD (*n* = 83)**	**Control (*n* = 29)**
Sex (male/female)	54/29	8/21
Age (years)	66.2 ± 7.4	65.4 ± 11.2
MDS diagnosis (established/probable)	76/7	-
Disease duration (years)	5.5 ± 4.8	-
Motor phenotype:	TD: 40	-
	PIGD: 33	
	I: 10	
MDS-UPDRS III score	29.6 ± 11.3	-
Hoehn & Yahr stage (taken as part of the MDS-UPDRS)	1.98 ± 0.6	-
MoCA score	25.7 ± 4.2[a]	26.6 ± 2.3[a]

Abbreviations: MDS diagnosis, Movement Disorders Society (MDS) diagnostic criteria for PD; Disease duration (years), duration of motor symptoms in years; TD, tremor dominant; PIGD, postural instability/gait difficulty; I, indeterminate; MDS-UPDRS III, International Parkinson and Movement Disorder Society Unified Parkinson's Disease Rating Scale Part III; MoCA, Montreal Cognitive Assessment.
Age, disease duration, MDS-UPDRS III score, Hohen & Yahr stage, and MoCA score are presented as mean ± standard deviation.
[a]MoCA scores were available from 58/83 individuals with PD and from 23/29 controls.

1032

Table 2: Linear mixed effects models of CI and CIV levels in single muscle fibers in individuals with PD and controls

	Dependent variable					
	log(NDUFB10/VDAC1)			**log(MTCO1/VDAC1)**		
Predictors	*B*	95% CI	*P*-value	*B*	95% CI	*P*-value
Disease state (PD)	-0.016	-0.047 – 0.014	0.290	-0.010	-0.050 – 0.029	0.609
Age	-0.002	-0.003 – -1.2e-04	**0.034**	-0.002	-0.004 – -2.5e-04	**0.026**
Sex (Male)	0.019	-0.007 – 0.045	0.153	0.052	0.018 – 0.086	**0.003**
Smoking	-0.005	-0.057 – 0.047	0.849	-0.020	-0.089 – 0.048	0.564
Batch (Batch 2)[a]	-0.102	-0.126 – -0.078	**<0.001**	0.064	0.032 – 0.095	**<0.001**
Random Effects						
σ^2	0.004			0.007		
$\tau_{00\ Subject}$	0.003			0.006		
ICC	0.479			0.439		
$n_{\ Subject}$	92			92		
Observations	9073			9073		
Marginal R^2 / Conditional R^2	0.305 / 0.638			0.107 / 0.499		

Abbreviations: log(NDUFB10/VDAC1), complex I level adjusted for mitochondrial content; log(MTCO1/VDAC1), complex IV level adjusted for mitochondrial content; *B*, regression coefficient (unstandardized); 95% CI, 95% confidence interval of the regression coefficient; σ^2, residual variance; $\tau_{00\ Subject}$, random intercept variance; ICC = intraclass correlation coefficient, representing the proportion of total variance in the dependent variable attributable to the grouping structure (i.e, subjects); $n_{\ Subject}$, number of study subjects.
Significant *P*-values are in bold. Nominal *P*-values are given.

[a]Immunohistochemistry staining was performed in two batches.

1033

Table 3: Linear regression models of enzymatic activity of CI, II, III, IV and citrate synthase in individuals with PD and controls

	Dependent variable														
	log(CI/CS)			**log(CII/CS)**			**log(CIII/CS)**			**log(CIV/CS)**			**log(CS)**		
Predictors	*B*	95% CI	*P*-value (adjusted)[a]	*B*	95% CI	*P*-value (adjusted)[a]	*B*	95% CI	*P*-value (adjusted)[a]	*B*	95% CI	*P*-value (adjusted)[a]	*B*	95% CI	*P*-value
Disease state (PD)	-0.079	-0.137 – -0.021	**0.008 (0.032)**	-0.043	-0.103 – 0.018	0.163 (0.313)	-0.038	-0.102 – 0.025	0.235 (0.313)	-0.027	-0.089 – 0.035	0.383 (0.383)	0.034	-0.090 – 0.159	0.582
Age	-0.001	-0.004 – 0.003	0.693	0.002	-0.001 – 0.006	0.143	0.008	0.005 – 0.011	**<0.001**	0.003	-1.8e-04 – 0.007	0.063	-0.001	-0.008 – 0.006	0.826
Sex (Male)	0.027	-0.027 – 0.082	0.323	0.013	-0.043 – 0.070	0.640	0.006	-0.052 – 0.064	0.846	0.017	-0.041 – 0.076	0.555	-0.023	-0.140 – 0.093	0.690
Batch (1-6)[b]	-	-	-	-	-	-	-	-	-	-	-	-	-	-	-
Observations	82			82			67[c]			82			82		
R^2 / R^2 adjusted	0.481 / 0.424			0.777 / 0.752			0.762 / 0.734			0.348 / 0.276			0.363 / 0.293		

Abbreviations: CI, complex I activity; CII, complex II activity; CIII, complex III activity; CIV, complex IV activity; CS, citrate synthase activity; x/CS, activity x (CI, CII, CIII, or CIV) normalized to citrate synthase activity; *B*, regression coefficient (unstandardized); 95% CI, 95% confidence interval of the regression coefficient.
Significant *P*-values are in bold. Nominal and adjusted *P*-values are given.

[a]Parentheses show *P*-values adjusted for multiple testing using the Benjamini-Hochberg procedure for four tests, i.e., CI/CS, CII/CS, CIII/CS and CIV/CS between the PD and control groups.
[b]Detailed coefficients for batch variables are provided in Supplementary Table 5a.
[c]Complex III activity measurements from 15 individuals were excluded from the analyses due to technical issues with the reduction of decylubiquinone.

1034